Biochemical Pharmacology 230 (2024) 116578

Contents lists available at ScienceDirect

Biochemical Pharmacology

journal homepage: www.elsevier.com/locate/biochempharm

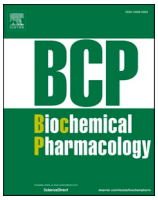

Ponatinib exacerbate renal injury in systemic lupus erythematosus mouse model through PDGFR-PI3K/AKT pathway

Yixin Dong [a,1], Gangan Wang [b,1], Xiwei Yan [b], Wenling Ye [b], Xiangyu Qiao [a], Xingyu Deng [a], Pengju Ren [a], Chunyu Jia [b], Gang Chen [b], Ke Zheng [b], Chengyu Jiang [a,*], Xuemei Li [b,*]

[a] State Key Laboratory of Common Mechanism Research for Major Diseases, Institute of Basic Medical Sciences, Chinese Academy of Medical Sciences & Peking Union Medical College, Beijing, China

[b] Department of Nephrology, Peking Union Medical College Hospital, Chinese Academy of Medical Sciences & Peking Union Medical College, Beijing, China

ARTICLE INFO

Keywords:
Ponatinib
Systemic lupus erythematosus
Tyrosine kinase inhibitors
Nephrotoxicity
Adiponectin

ABSTRACT

Lupus nephritis (LN) is a common clinical complication of systemic lupus erythematosus (SLE). Proliferative lupus nephritis represents the gravest form of LN, and since effective drugs for its treatment are still lacking, tyrosine kinase inhibitors (TKIs) find extensive clinical utility due to their notable impact on suppressing cell proliferation and may serve as potential drugs for LN treatment. However, previous studies on the effects of TKI on LN have been controversial. Ponatinib, a third-generation TKI, lacks studies on its role in LN. This study aimed to investigate the impact of the ponatinib on LN. MRL/lpr mice were evaluated for renal function, autoimmune markers and histopathological changes after oral administration of ponatinib. RNA-seq analysis was performed to explore the molecular pathways involved in ponatinib-induced kidney injury. Ponatinib uniquely exacerbated renal damage in MRL/lpr mice, evidenced by a decline in renal function and acute pathological changes, without affecting lupus-related autoimmune markers. Differential expressed genes analysis and functional enrichment implicate ponatinib-induced renal damage in MRL/lpr mice associated with adiponectin. Furthermore, we verified ponatinib signaling the PI3K/AKT pathway through PDGFRα, potentially influencing high molecular weight adiponectin (HMW ADIPOQ) expression and exacerbating renal damage. In conclusion, this study demonstrates that ponatinib can up-regulate HMW ADIPOQ expression via the PI3K/AKT pathway by inhibiting PDGFRα phosphorylation, highlighting the potential nephrotoxic effects of ponatinib in lupus-prone mice, and underscoring the importance of monitoring renal function in systemic autoimmune diseases patients receiving ponatinib.

1. Introduction

Systemic lupus erythematosus (SLE) is a chronic autoimmune disease, is marked by ongoing inflammation and damage to multi-pleorgans. Lupus nephritis (LN) is a common clinical complication of SLE, and the clinical manifestations are highly heterogeneous, ranging from mild proteinuria to nephrotic-range proteinuria, affecting 30–60 % of adults and up to 70 % of children with SLE [1,2].

LN typically presents with glomerular inflammation, tubular damage, and interstitial lymphocyte infiltration. The common

Abbreviations: SLE, Systemic lupus erythematosus; LN, Lupus nephritis; TKIs, Tyrosine kinase inhibitors; PDGFR, platelet-derived growth factor receptor; RET, rearranged during transfection; KIT, kinase insert domain receptor; FLT3, FMS-like receptor tyrosine kinase-3; SRC, SRC proto-oncogene, non-receptor tyrosine kinase; FGFR, fibroblast growth factor receptor; VEGFR, vascular endothelial growth factor receptor; Adipoq, Adiponectin; dsDNA, double stranded DNA; ANA, anti-nuclear antibody; C3, Component 3; HRP, horseradish peroxidase; TMB, 3,3′,5,5′-Tetramethylbenzidine; BUN, blood urea nitrogen; Cr, Creatinine; UPCR, urine protein/creatinine ratio; H&E, hematoxylin and eosin; PAS, periodic acid-Schiff; PASM, Periodic-acid silver methenamine; TEM, Transmission electron microscopy; DEGs, Differential Expressed Genes; GO, gene ontology; PPI, protein-protein interaction; p-PDGFRα, phosphorylated Platelet-Derived Growth Factor Receptor α; PDGFRα, Platelet-Derived Growth Factor Receptor α; p-AKT, phosphorylated Protein Kinase B; AKT, Protein Kinase B; HMW, high molecular weight; mIHC, multiplex Immunohistochemistry; PPARγ, Peroxisome Proliferator-Activated Receptor γ; AP, adipocyte progenitor cells; RTKs., receptor tyrosine kinases; PBMCs, Peripheral Blood Mononuclear Cells; IL-8, Interleukin-8; MCP-1, Monocyte Chemoattractant Protein-1; LMW, low-molecular-weight.

* Corresponding authors.
E-mail addresses: jiang@pumc.edu.cn (C. Jiang), lixmpumch_kidney@outlook.com, lixm@pumch.cn (X. Li).

[1] Contributed equally to this work.

https://doi.org/10.1016/j.bcp.2024.116578
Received 3 May 2024; Received in revised form 12 October 2024; Accepted 15 October 2024
Available online 19 October 2024

histopathological manifestations of LN include membranous glomerulonephritis, proliferative glomerulonephritis, and mixed-type glomerulonephritis. And proliferative lupus nephritis is the most severe form of lupus nephritis [3]. Typically occurring early in the course of SLE, three years after and usually within five years of the onset of SLE, LN represents a significant complication associated with an unfavorable prognosis in patients with lupus, being a major contributing factor to SLE lethality. The management of LN often relies on immunosuppressive drugs, although these treatments are not uniformly effective. The various comorbidities associated with immunosuppressive treatment, such as infections, osteoporosis and cardiovascular and reproductive effects, remain a concern [4].

Tyrosine kinase inhibitors (TKIs), widely recognized for their substantial inhibition of cell proliferation, have emerged as an extensively utilized class of drugs, owing to their prolonged and diverse applications [5]. They are increasingly pivotal in treating a spectrum of tumors and autoimmune diseases [6]. It has been shown that SLE patients have abnormally enhanced primary monocyte chemotaxis, and after administration of TKI the abnormal migration was restored to normal levels [7]. Animal studies also have illuminated the potential of imatinib (a first-generation TKI) in ameliorating renal damage in lupus-prone mice, significantly retarding the progression of proteinuria, and averting renal functional impairment [8–10]. But multiple investigations suggest an association between diverse TKIs and renal injury [11–14]. This association encompasses glomerular diseases and renal dysfunction, potentially involving a myriad of underlying mechanisms.

Ponatinib, a third-generation TKI, has a broader spectrum of tyrosine kinase inhibitory effects compared to imatinib, including stronger inhibition of platelet-derived growth factor receptor (PDGFR). Therefore, it may show better efficacy in treating certain tumors associated with PDGFR [15,16]. It is employed to combat resistance caused by the BCR-ABL kinase T315I mutation [17] and is widely acknowledged as one of the most efficacious TKIs for leukemia treatment. Ponatinib is known to target not only BCR-ABL but also members of the rearranged during transfection (RET), FMS-like receptor tyrosine kinase-3 (FLT3), kinase insert domain receptor (KIT), SRC proto-oncogene, non-receptor tyrosine kinase (SRC), fibroblast growth factor receptor (FGFR), vascular endothelial growth factor receptor (VEGFR), and PDGFR families. Few cases have reported renal injury in some patients using ponatinib, and the underlying mechanism remains unclear [12,18]. Although the summary of product characteristics has not identified any signals of nephrotoxicity associated with ponatinib, the exact reasons for these observations are still to be determined. From our knowledge, as of now, there is a lack of research demonstrating the role of ponatinib in the effect of lupus nephritis. Here, this study aimed to investigate the impact of ponatinib on lupus nephritis and reveal the mechanisms underlying kidney injury, with the aspiration of providing a new insight for the clinical application of ponatinib.

2. Method

2.1. Mice

Female MRL/lpr and C57BL/6 mice aged 6–8 weeks were purchased from SPF (Beijing) Biotechnology Co., Ltd. Age-matched female MRL/MpJ mice were obtained from Cyagen Biosciences Inc. All mice were housed under specific pathogen-free conditions, maintained on a 12/12-hour light/dark cycle, and had ad libitum access to water and standard rodent chow at the Center for Experimental Animal Research of Peking Union Medical College.

2.2. Experimental design

Ponatinib (BCP02037, CAS: 943319–70-8, Biochempartner Co., Ltd.) was dissolved in ddH_2O to prepare stock solution of 10 mg/mL. Prednisone Acetate (H33021207, Shandong Xinhua Pharmaceutical Co., Ltd.) was dissolved in ddH_2O to make solution (1 mg/mL) and stored at −20 °C. GW9662(HY-16578, CAS: 22978-25-2, MCE.) was prepared as a solution at a concentration of 1 mg/mL using a mixture of 10% DMSO and 90% Corn Oil. These solutions were aliquoted and stored at −20 °C.

For *in vivo* the drug efficacy, 30 mice of the three genotypes were divided into six groups as follows: MRL/lpr-H_2O; MRL/lpr-PONA; C57-H_2O; C57-PONA; MRL/MpJ-H_2O; MRL/MpJ-PONA. Mice in MRL/lpr-PONA, C57-PONA and MRL/MpJ-PONA were treated with daily oral intragastric administration of ponatinib at a dose of 0.01 mg/g/d [19] for 8 weeks. The remaining mice received ddH_2O alone.

For experiments investigating dose dependence with ponatinib, five groups were established, total comprising 25 female MRL/lpr mice: Blank (ddH_2O, n = 5), Prednisone (PD, 0.005 mg/g/d, n = 5), High-dose Ponatinib (HP, 0.03 mg/g/d, n = 5), Medium-dose of Ponatinib (MP, 0.01 mg/g/d, n = 5), low-dose of Ponatinib (LP, 0.003 mg/g/d, n = 5). Treatment duration was 8 weeks.

In the experiments to verify the role of Adiponectin (Adipoq), we established three groups, each consisting of five MRL/lpr mice: Blank (ddH_2O, n = 5), Ponatinib (0.02 mg/g/d, n = 5), and Ponatinib + GW9662 (Ponatinib: 0.02 mg/g/d, GW9662: 1 μg/g, n = 5). The treatment duration was two weeks. All animals were healthy at the start of the experiment. The mice were anesthetized with tribromoethanol (30 μL/g, MA0478, Meilun Bio) for the experiments.

2.3. Enzyme-linked immunosorbent assay (ELISA)

The Mouse anti-double stranded DNA (dsDNA) antibody ELISA kit (CSB-E12911m) and the Mouse anti-nuclear antibody (ANA) ELISA Kit (CSB-E12912m) were obtained from CUSABIO Technology LLC. The Mouse Complement Component 3 (C3) ELISA Kit (SEA861Mu) was acquired from Cloud-Clone Corp. In accordance with the manufacturer's guidelines, serum from mice was diluted at the following ratios: 1:5 for dsDNA antibody, 1:200 for ANA, and 1:5000 for C3. In brief, the diluted serum samples were added to the provided microtiter plate wells in each kit. Then, biotin-conjugated antigen and horseradish peroxidase (HRP) were introduced into each well and incubated. 3, 3′,5,5′-Tetramethylbenzidine (TMB) substrate solution was subsequently added to all wells. The enzyme-substrate reaction was stopped upon color change occurrence. The resulting color change was measured spectrophotometrically at 450 nm.

2.4. Evaluation of renal injury

To assess kidney damage of mice, we collected urine and serum samples for laboratory testing. Additionally, we computed the kidney index, which was calculated as the ratio of kidney weight to body weight. The total protein content in urine was quantified using the Bradford Protein Assay Kit (PC0010, Beijing Solarbio Science & Technology Co., Ltd). The blood urea nitrogen (BUN) concentration in serum was measured using the Blood Urea Nitrogen Assay Kit (C013-1–1, Nanjing Jiancheng Bioengineering Institute). Additionally, the concentrations of creatinine in both serum and urine were determined using a Creatinine (Cr) Assay kit (C011-2–1, Nanjing Jiancheng Bioengineering Institute). The urine protein/creatinine ratio (UPCR) was used to estimate the extent of urinary protein excretion.

2.5. Renal histology

Mice were anesthetized using isoflurane, followed by perfusion with saline through the heart. Kidney tissues were isolated and fixed in 4 % paraformaldehyde. Conventional paraffin fixation methods were employed to fix kidney sections (2 μm thick), which underwent staining with hematoxylin and eosin (H&E), periodic acid-Schiff (PAS), Periodic-acid silver methenamine (PASM) and Masson stains for subsequent histological examination. Renal histologic evaluation of lupus nephritis activity index was conducted according to the National Institutes of

Health indices [20] The histopathological scores were assigned by two pathologists in a blinded fashion

2.6. Multiplex immunohistochemistry

Paraffin-fixed kidney sections (3 μm thick) were used for immunofluorescence staining. The slides were deparaffinized using xylene, followed by rehydration in histological-grade ethanol. Subsequently, fixation was carried out using 3 % hydrogen peroxide in methanol. Antigen retrieval was performed using pH 9.0 EDTA buffer. The primary antibodies used were HRP-Goat anti mouse IgM mu chain (1:100, BF03006, Biodragon), HRP Goat Anti-Mouse IgG (H + L) (1:100, AS003, ABclonal), C3/C3b/C3c Polyclonal antibody (1:1000, 21337–1-AP, Proteintech.). Tyramide signal amplification (TSA) visualization was done using the Opal 6-Plex Detection Kit (formerly Opal 7-Color Automation IHC Kit) (no. NEL821001KT, Akoya Biosciences). Opal 520 (1:100), Opal 570 (1:100), Opal 620 (1:100), and Opal 690 (1:100) were used to pair primary antibodies. Performing multiplex staining according to the machine's preset program. The slides were counterstained with Spectral DAPI (Akoya Biosciences) and mounted using a durable aqueous-based mounting medium.

2.7. Multispectral image acquisition and analysis

The Vectra 3 Automated Quantitative Pathology Imaging System from Akoya Biosciences was utilized for section processing. Glomerulus were acquired at 40 × original magnification. Signals for IgM, IgG, C3 and DAPI were visualised using inForm Tissue Finder software 2.4.9 (Akoya Biosciences). Immune deposits in kidney were quantified by densitometry analysis. For each section, 5 high-power fields were randomly selected and all glomeruli within the high-power field were counted. Three mice were counted in each group. ImageJ software (NIH, USA) was used to measure signal intensities.

2.8. Transmission electron microscopy

Kidney sections were examined by electron microscopy to assess ultrastructural changes. Renal samples (60 nm) were made into ultrathin sections after fixation with 2.5 % glutaraldehyde and post-fixation with 1 % osmium acid. Transmission electron microscopy (TEM, TEM-1400plus) was use for observation and capturing images.

2.9. Kidney tissue RNA-seq and data analysis

RNA-seq was performed by Beijing Berry And Kang Biotechnology Co., Ltd. The experiment followed our laboratory's routine procedures [21]. RNA purity and concentration were examined, followed by measuring RNA integrity and quantity. Qualified samples were used for constructing libraries. RNA libraries were generated using the Hieff NGS® Ultima Dual-mode mRNA Library Prep Kit for Illumina (12301ES96 Yeasen) following the manufacturer's recommendations. After library preparation and pooling of different samples, the samples underwent Illumina sequencing.

Quality control for sequencing data employed FastQC (version 0.11.2). Subsequently, adapters were eliminated, and sequences with low-quality scores were filtered out. For transcriptome sequencing data, TopHat (version 2.0.11) was employed to align reads to the mouse genome. (UCSC mm39, https://genome.ucsc.edu/cgi-bin/hgTracks?db = mm39&position = lastDbPos) Reads assigned to different genes were quantified using featureCounts (version 2.0.1).

2.10. Calculation of differential expressed genes (DEGs) and pathway enrichment analysis

DEGs were computed from gene expression read counts matrices using DESeq2 (version 1.28.1) and DEGseq (version 1.42.0) in R (version 4.0.0). Genes with adjusted *P*-value < 0.05.

Genes with a fold change greater than 2 or less than 0.5 were recognized as differentially expressed genes (DEGs). Pathway clustering and gene ontology (GO) enrichment analyses of DEGs were carried out using the MetaCore Database (Clarivate Analytics, USA, https://portal.genego.com/). Bioinformatics (https://www.bioinformatics.com.cn/plot_basic_GO_term_bp_cc_mf_bar_plot_04 6) were used to visualize the clustered GO result. The visualization of clustered pathways was conducted using Cytoscape (version 3.8.0) in conjunction with EnrichmentMap (version 3.1.0). A protein–protein interaction (PPI) network was established using the STRING (http: //string.embl.de/) database. After obtaining the protein–protein interaction (PPI) relationships, a network diagram was created utilizing Cytoscape (version 3.8.0) software.

2.11. Western blot

Western blot analysis was employed to assess the expression levels of phosphorylated Platelet-Derived Growth Factor Receptor α / Platelet-Derived Growth Factor Receptor α (p-PDGFRα/PDGFRα), phosphorylated Protein Kinase B / Protein Kinase B (p-AKT/AKT), and Adiponectin (ADIPOQ) protein expression in the kidney. The experiment followed standard protocols. Briefly, 45 μg of kidney protein samples were separated on a FuturePAGE™ 4–12 % 15 Wells (ET15412Gel, ACE Biotechnology) using MOPS-SDS Running Buffer (BR0001-02, ACE Biotechnology). Proteins were then transferred onto a PVDF membrane. Protein loading quantification was performed using Revert 700 Total Protein Stain (926–11015, LI-COR). After 30 min of blocking with Rapid Blocking Buffer (RM02956, ABclonal), primary antibodies [PDGFR-α (phospho Tyr754) Polyclonal Antibody (1:500, AP0993 AbBox,); PDGFR alpha Rabbit pAb (1:500, A2103 ABclonal); Phospho-AKT1-S473 Rabbit mAb (1:500, AP0637 ABclonal); Pan-Akt Rabbit mAb (1:2000, A18675 ABclonal); Adiponectin Rabbit mAb (1:500, A23473 ABclonal)] were added and incubated overnight at 4℃. Subsequently, a secondary antibody [HRP-labeled Goat Anti-Rabbit IgG (H + L) (1:5000, AS014 ABclonal)] was incubated at 4℃ for 1.5 h. Protein signals were detected using the ECL kit (WBKLS0500, Millipore).

Expression levels of high molecular weight (HMW) ADIPOQ in the kidney were detected by western blot with 4–12 % NativePAGE Gels (36249ES10, Yeasen) with Precast Running Buffer for Native PAGE (36258ES05, Yeasen) as electrophoresis solution. The remaining steps were the same as described above. ImageJ software (NIH, USA) was used for quantification and normalization of the target protein.

2.12. q-PCR analysis

RNA was extracted from TRIzol (15596026CN, Thermo Fisher Scientific) to quantify the expression of *Adipoq* in three mouse genotypes. Reverse transcription utilized HiScript Reverse Transcriptase (R111, Vazyme), and real-time qPCR was performed using 2 × Taq Master Mix (P111-01, Vazyme). Mouse *β-actin* served as a reference gene. The primer sequences used were as follows:

Adipoq Forward: 5′-TGT TCC TCT TAA TCC TGC CCA-3′;
Adipoq Reverse: 5′-CCA ACC TGC ACA AGT TCC CTT-3′;
β-actin Forward: 5′-CAT TGC TGA CAG GAT GCA GAA GG-3′;
β-actin Reverse: 5′-TGC TGG AAG GTG GAC AGT GAG G-3′.

2.13. Statistical analysis

All experimental data were expressed as mean ± SEM. All experiments were repeated at least twice. To assess the difference between experimental and control groups, a Student's T-test was employed. When there were more than two experimental conditions, statistical significance was determined using one-way ANOVA (Nonparametric or Mixed) with Dunnett's multiple comparisons test. For survival curve analysis, the Log-RANK (Mantel-Cox) test was utilized. All statistical

analysis and graphing for each experiment were conducted using GraphPad Prism software.

3. Result

3.1. Ponatinib uniquely exacerbates renal injury in MRL/lpr mice

To investigate the potential impact of ponatinib on LN, we administered ponatinib to MRL/lpr mice, a spontaneous mice model of LN. Based on previous research [19], we selected an experimental dose of 0.01 mg/g of ponatinib, and a treatment duration of 8 weeks (Fig. 1A). MRL/lpr mice treated with ponatinib exhibited elevated levels of serum UPCR (Fig. 1B, $p = 0.0461$), BUN (Fig. 1C, $p = 0.0375$), and Scr (Fig. 1D, $p = 0.0380$), compared to those treated with water. Ponatinib significantly increased the kidney index of MRL/lpr mice compared to the ddH_2O group (Fig. 1E, $p = 0.034$). These finding suggest that ponatinib exacerbates kidney damage in MRL/lpr mice. To explore whether ponatinib-induced renal damage is unique to lupus-prone mice, we separately administered ponatinib to C57 mice and MRL/MpJ mice (the parent and control strain for MRL/lpr mice). The results revealed that, compared to those not receiving ponatinib, both C57 and MRL/MpJ mice showed no significant differences in Scr (Fig. 1D, C57-H2O vs C57-PONA, $p = 0.145$; MRL/ MpJ –H_2O vs MRL/ MpJ –PONA, $p = 0.3355$), and UPCR (Fig. 1B, C57-H2O vs C57-PONA, $p = 0.5049$; MRL/ MpJ –H_2O vs MRL/ MpJ –PONA, $p = 0.0511$). Serum BUN levels decreased in the C57 and MRL/ MpJ groups after administration of ponatinib (Fig. 1C). For C57 and MPJ mice, administration of ponatinib also had no effect on their kidney indexes (Fig. 1E, C57-H2O vs C57-PONA, $p = 0.149$; MRL/MpJ-H_2O vs MRL/MpJ-PONA, $p = 0.1178$).

To further verify the nephrotoxic effects of ponatinib, we conducted histopathological examinations of the mice kidneys. Histopathological examination of kidney tissues indicates a predominance of acute lesions in MRL/lpr mice treated with ponatinib (Fig. 2A). The lupus nephritis activity score (Fig. 2H) during the acute phase revealed significant differences between the two groups in terms of cellular/fibrocellular crescents (Fig. 2B), endocapillary hypercellularity (Fig. 2C), fibrinoid necrosis (Fig. 2D) and neutrophil/karyorhexis (Fig. 2E). However, no apparent distinctions were observed between the groups in terms of hyaline thrombi (Fig. 2F) and interstitial inflammation (Fig. 2G). In contrast, when comparing mice that received ponatinib to those that did not, both C57 and MRL/MpJ mice showed no apparent signs of renal damage, with no observable histopathological alterations. Electron microscopy revealed electron-dense deposits in the glomerulus, primarily in the mesangial area, beneath endothelial cells, and beneath epithelial cells. Features of podocyte injury, such as foot process fusion, were also evident [4]. Electron microscopy revealed widespread foot process fusion and extensive damage to the endothelial cells of the glomerular capillaries in the ponatinib treated group (Fig. 2I).

3.2. Ponatinib does not induce an increase in autoimmune activity

To elucidate the underlying cause of kidney damage in MRL/lpr mice treated with ponatinib, we assessed serum autoimmune parameters related to LN. Specifically, we measured serum levels of dsDNA and ANA, which are indicative of autoimmune activity in mouse strains. Surprisingly, we found no statistically significant differences in serum ANA (Fig. 3A, $p = 0.4537$) and dsDNA levels (Fig. 3B, $p = 0.4693$) between ponatinib-treated mice and those treated with ddH_2O. The level of serum C3 (Fig. 3C, $p = 0.0440$) exhibited significant difference between the two groups. For the C57 group of mice, administration of ponatinib increased their serum ANA levels, while it had no effect on MRL/MpJ mice (Fig. 3A, C57-H2O vs C57-PONA, $p = 0.0349$; MRL/ MpJ-H_2O vs MRL/MpJ-PONA, $p = 0.264$).

To investigate whether there was an elevation in local autoimmune activity within the kidneys, we conducted multiplex Immunohistochemistry (mIHC) for IgG, IgM, and C3 on the kidneys of MRL/lpr mice

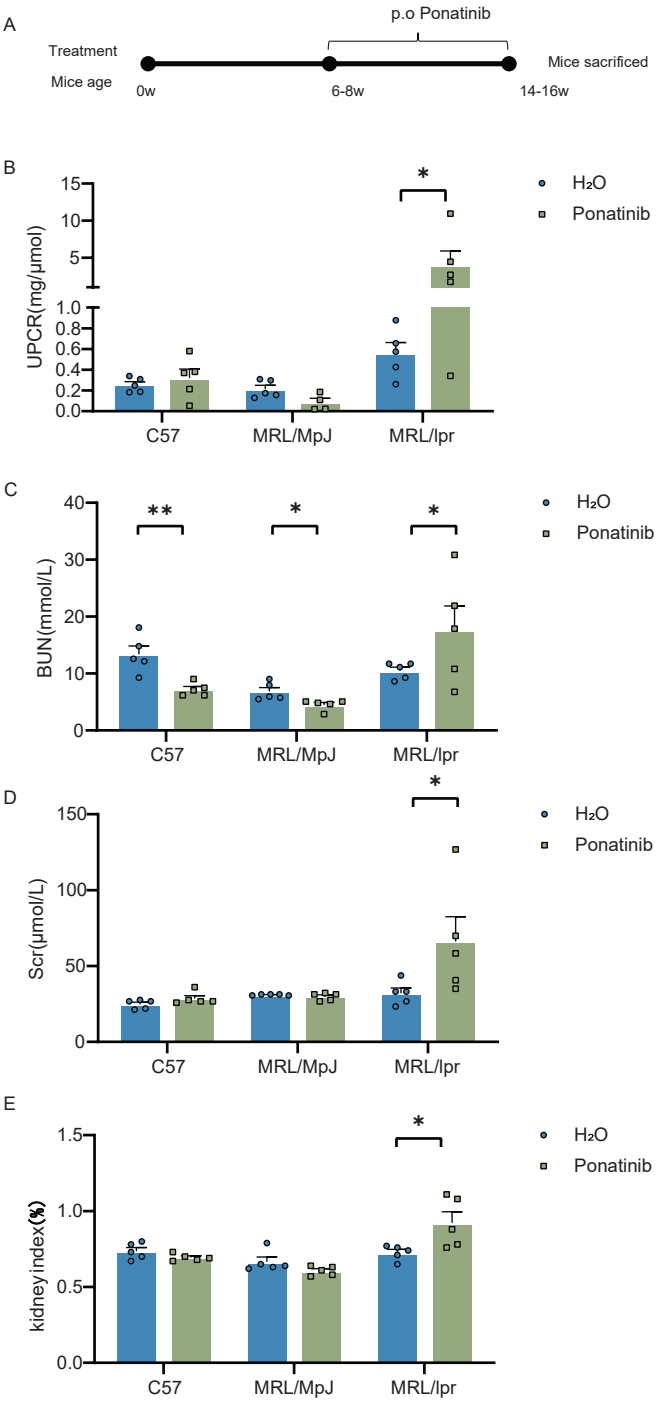

Fig. 1. Kidney Dysfunction in Ponatinib-Treated MRL/lpr Lupus Mice, with No Impact on MRL/MpJ and C57 Mice. (A) Overview of the experimental design. (B) Urine protein-to-creatinine ratio, (C) Blood urea nitrogen, (D) serum creatinine results and (E) Kidney index after 8 weeks of ponatinib administration in the three mouse groups. The data are presented as the mean ± SEM. *p < 0.05; * *p < 0.01; * **p < 0.001 versus the corresponding control groups.

treated with ponatinib (Fig. 3D). Interestingly, the results revealed consistent patterns in kidney deposition of IgG, IgM, and C3 between MRL/lpr mice receiving ponatinib and those receiving ddH_2O, without statistically significant differences (Fig. 3E-G). This outcome suggests that the kidney damage induced by ponatinib in MRL/lpr mice is not associated with an augmentation in local autoimmune activity. Thus, ponatinib might contribute to renal injury through alternative mechanisms.

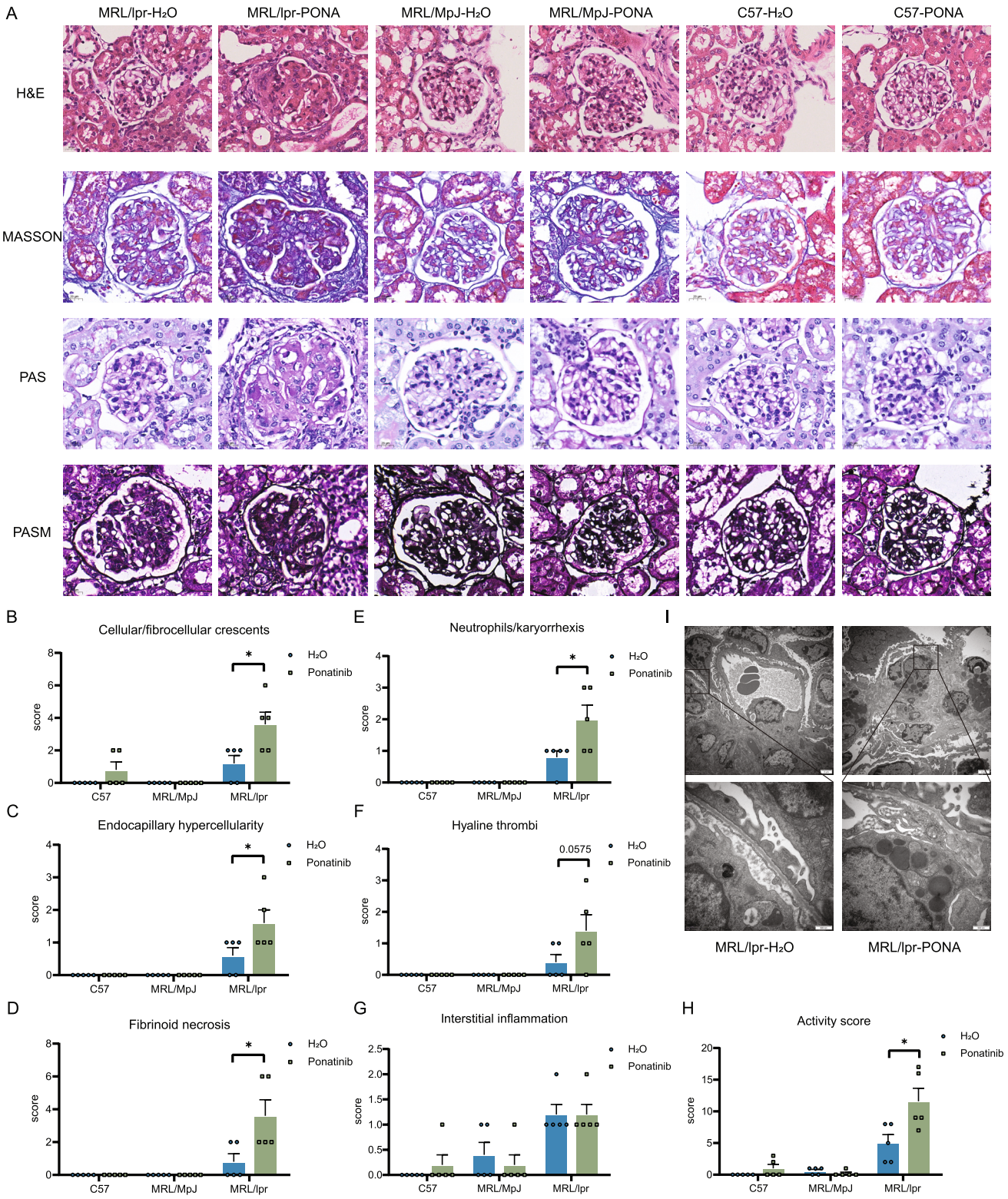

Fig. 2. Renal Histopathological Results in MRL/lpr Lupus Mice, MRL/MpJ Mice, and C57 Mice Treated with Ponatinib. (A) Histological staining results (HE, Masson, PAS, PASM) of renal glomerular tissue (40X magnification). (B) Cellular/fibrocellular crescents score, (C) Endocapillary hypercellularity score, (D) Fibrinoid necrosis score, (E) Neutrophils/karyorhexis score, (F) Hyaline thrombi score, (G) Interstitial inflammation score and (H) Renal activity score; (I) Electron microscopy results. The data are presented as the mean ± SEM. *p < 0.05; * *p < 0.01; * **p < 0.001 versus the corresponding control groups.

3.3. Ponatinib-induced kidney damage is related to dose

Furthermore, to investigate the effects of ponatinib at varying doses, we used prednisone (0.005 mg/g) as a positive control, to evaluate the potential bidirectional effects of ponatinib at these doses, and to delineate the dose-dependent effects of ponatinib within the context of our experimental model (Fig. 4). However, the experimental results indicated that even low doses of ponatinib can cause damage to MRL/lpr

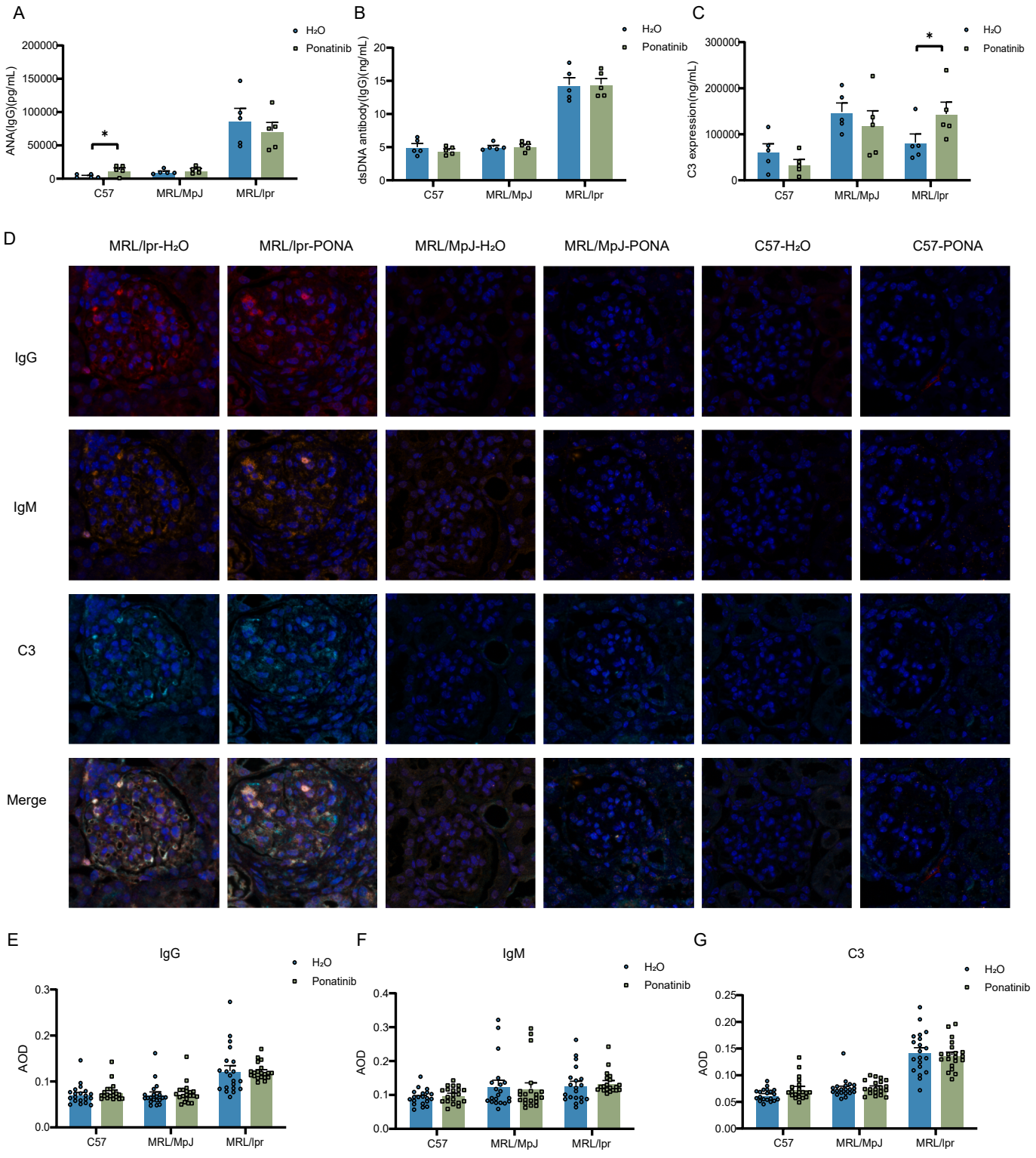

Fig. 3. Immunohistochemistry and Autoimmune Markers in Kidneys of Ponatinib-Treated MRL/lpr Lupus Mice, MRL/MpJ Mice, and C57 Mice. (A-C) Serum levels of ANA, dsDNA, and C3. (D) Immunofluorescence staining of kidney tissues; (E-G) Quantitative analysis of immunofluorescence staining in the kidneys; The data are presented as the mean ± SEM. *p < 0.05; * *p < 0.01; * **p < 0.001 versus the corresponding control groups.

mice. With an increase in the dose of ponatinib, kidney damage in MRL/lpr mice gradually escalated, and mice in the high-dose group began to die at the 4th week of administration. The results showed that mice in the high-dose ponatinib group began to die on the 30th day of administration. By the 36th day, all five mice in the high-dose ponatinib group had died. However, no mice in the medium or low-dose groups died during the 8-week experiment (Fig. 4A). These findings strongly suggest that ponatinib-induced renal damage is specific to the spontaneous lupus model in MRL/lpr mice. At the end of the 8-week trial, serum kidney biochemical indicators in surviving mice from each group were examined (Fig. 4B-E). Under low-dose ponatinib intervention, the kidney index ($p = 0.0487$) and urine protein/creatinine ratio ($p < 0.001$) of

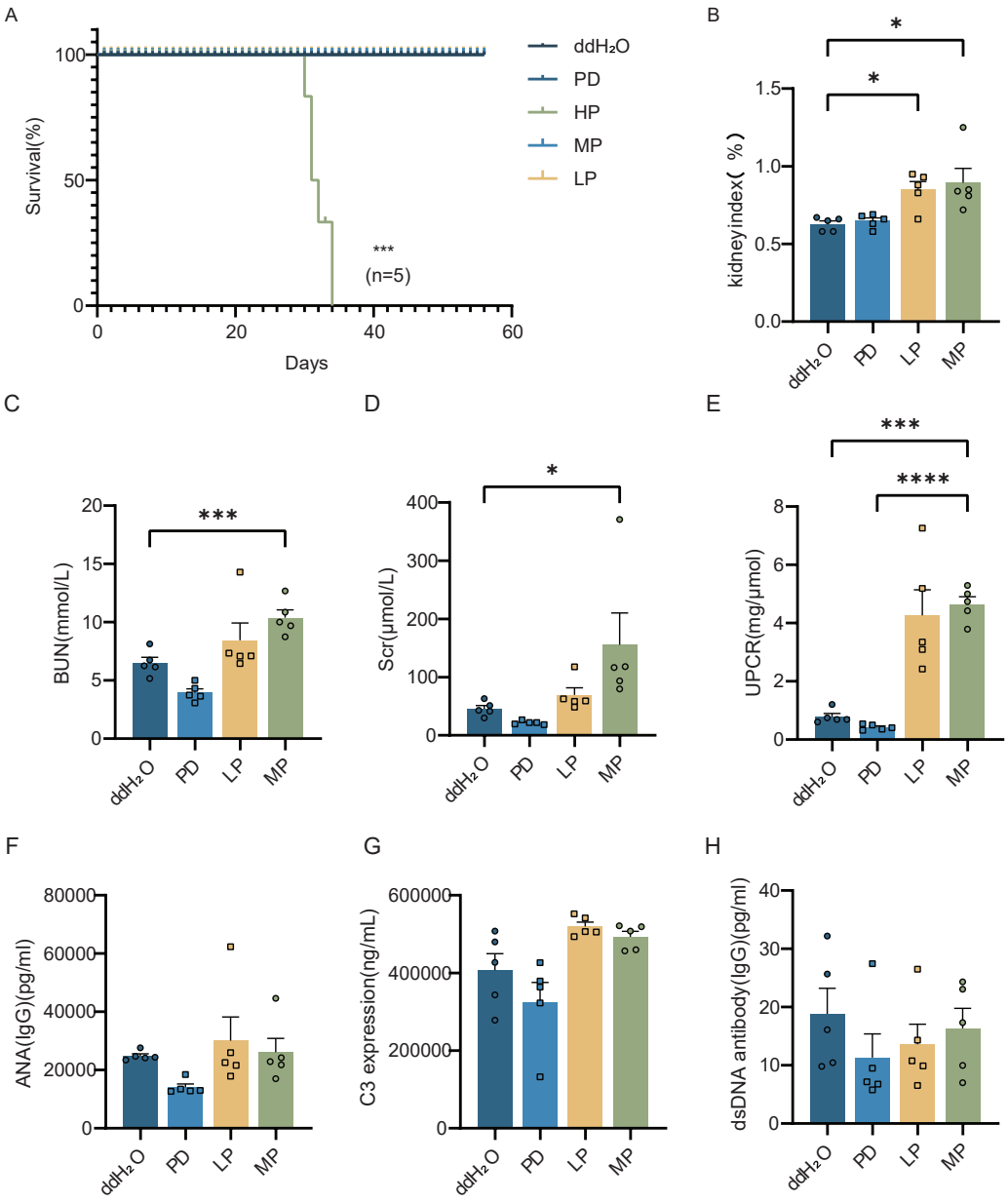

Fig. 4. Dose-dependent experiments reveal that Ponatinib-Induced Kidney Damage is Dose-Related. (A) Survival curves for MRL/lpr mice in each group. (B) Kidney index.(C-E) Serum levels of BUN, Scr, UPCR level. (F-H) Serum levels of ANA (Antinuclear Antibody), C3, and anti-dsDNA (anti-Double-Stranded DNA). The data are presented as the mean ± SEM. *p < 0.05; * *p < 0.01; * **p < 0.001 versus the corresponding control groups.

MRL/lpr mice were significantly increased compared to the control group, but there was only an upward trend in blood urea nitrogen and serum creatinine without statistical significance. The results of the medium-dose ponatinib group were consistent with previous experiments. After 8 weeks of intervention with 0.01 mg/g ponatinib, there was a significant increase in serum creatinine ($p = 0.0392$) and blood urea nitrogen ($p = 0.0251$) content in mice, with a statistically significant difference compared to the ddH_2O group ($p < 0.001$). Urinalysis results showed that, compared to the ddH_2O group, the urine protein-to-creatinine ratio was significantly increased ($p < 0.001$), and the kidneys were noticeably enlarged ($p = 0.0158$), indicating that 0.01 mg/g ponatinib caused significant kidney damage. Results related to autoimmune indicators were also consistent with previous experiments (Fig. 4F-H): ponatinib did not significantly affect autoimmune-related indicators in MRL/lpr mice, and there were no significant changes in serum ANA, anti-dsDNA antibody, and complement C3 levels in both the low-dose and medium-dose groups.

3.4. DEGs analysis and functional enrichment implicate ponatinib-induced renal damage in MRL/lpr mice associated with adiponectin

To investigate the underlying mechanism of renal injury by ponatinib in MRL/lpr mice, we conducted RNA sequencing of renal tissues from MRL/lpr-H_2O and MRL/lpr-PONA mice. Comparative analysis revealed that the MRL/lpr group exhibited altered expression in 44 genes, including 23 up-regulated and 21 down-regulated genes (Fig. 5A). To predict the biological-functional relationships of DEGs, we performed pathway enrichment analysis (Fig. 5B-C) and GO (Fig. 5D) analyses of DEGs. Pathway enrichment analysis using the Metacore database highlighted pathways associated with lipid metabolism, with top results including "Development_Differentiation of white adipocytes," "Development_Fetal brown fat cell differentiation," and "Development_Insulin, IGF-1, and TNF-alpha in brown adipocyte differentiation"(Fig. 5C). Visualization of the result of pathway enrichment analysis using the Enrichment Map plugin in Cytoscape indicated a

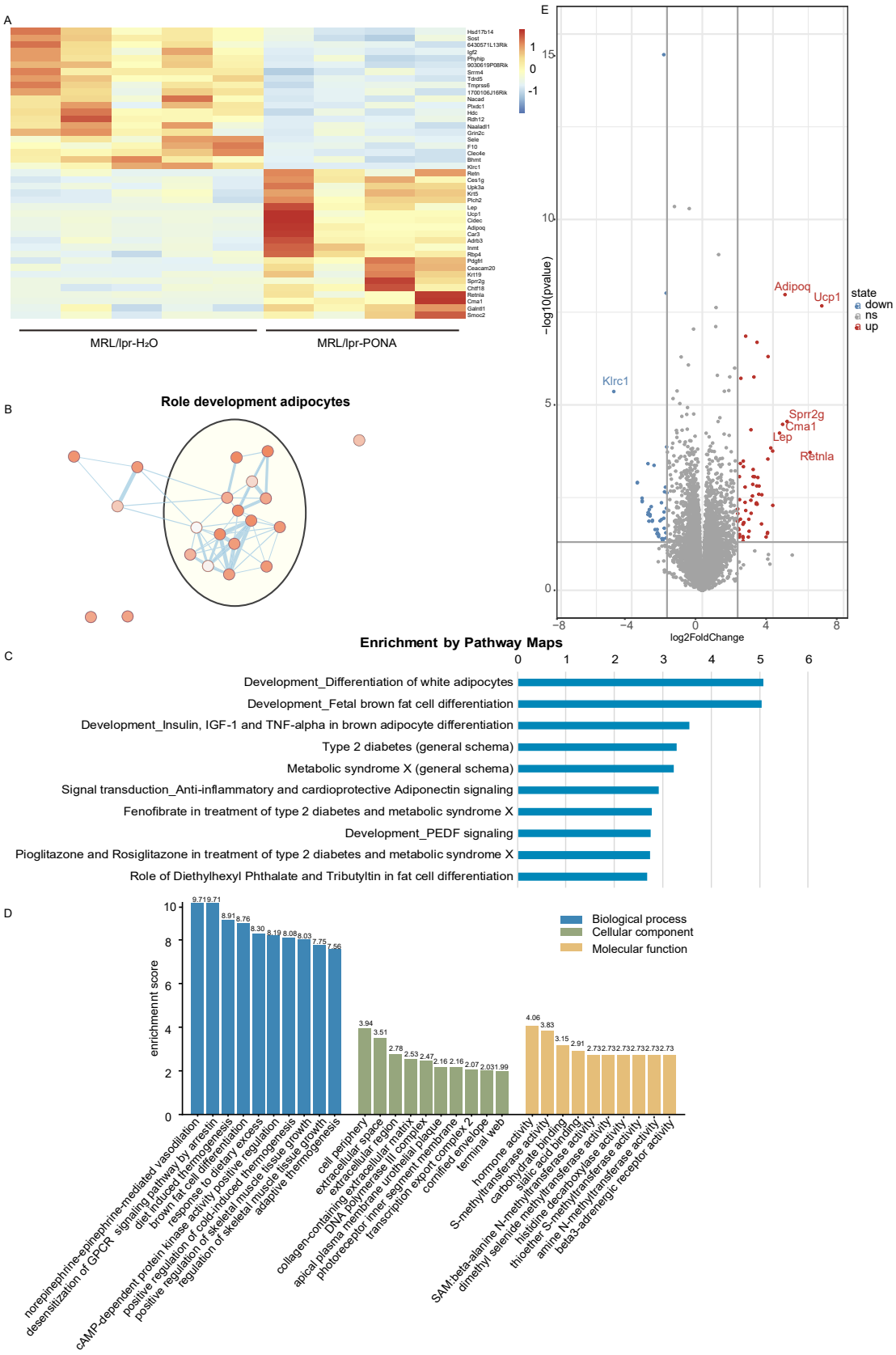

Fig. 5. RNA-seq and Pathway Enrichment Analysis of Kidneys from Ponatinib-Treated MRL/lpr Lupus Mice Suggests Association between Renal Injury and Lipid Metabolism. (A) Heatmap of Differentially Expressed Genes (DEGs) in kidney; (B) Functional enrichment visualized using the Enrichment Map application in Cytoscape; (C) Functional enrichment of the top 10 significant pathways for DEGs; (D) The GO analysis for DEGs; (E) Volcano plot of DEGs in kidney. The data are presented as the mean ± SEM. *p < 0.05; * *p < 0.01; * **p < 0.001 versus the corresponding control groups.

predominant association of pathways with adipocyte development (Fig. 5B). The GO analysis results indicate that these differentially expressed genes are involved in biological processes such as "norepinephrine-epinephrine-mediated vasodilation involved in regulation of systemic arterial blood pressure", "diet induced thermogenesis" "brown fat cell differentiation" "adaptive thermogenesis" (Fig. 5D).

Seven genes with over 20-fold expression changes in DEGs were identified (Fig. 4E), namely *Ucp1, Retnla, Sprr2g, Adipoq, Cma1, Lep, and Klrc1*. Among these, Adipoq stood out due to its known role as a crucial cytokine produced by adipocytes, closely linked to inflammation (see Table 1). Previous studies have demonstrated a significant elevation in plasma and urine levels of adiponectin in patients with renal involvement in SLE [22,23].Therefore, we hypothesized that ponatinib may exacerbate renal injury by influencing adiponectin expression.

3.5. Adiponectin causes kidney damage in MRL/lpr mice

To confirm the in vivo damaging effects of adiponectin, three groups of animals were treated with H_2O, Ponatinib, and Ponatinib plus GW6992. GW6992 is a commonly used Peroxisome Proliferator-Activated Receptor γ (PPARγ) antagonist that can inhibit the production of Adipoq [24]. The experimental results indicated that GW6992 significantly reduced the ponatinib-induced increases in BUN ($p < 0.001$, Fig. 6A), Scr ($p < 0.05$, Fig. 6B), UPCR ($p < 0.001$, Fig. 6C), and kidney index ($p < 0.001$, Fig. 6D) in MRL/lpr mice. The UPCR, BUN, Scr, and kidney index in the Ponatinib + GW6992 group were not significantly different from those in the blank group (Fig. 6A-D). This suggests that inhibiting the production of adiponectin can prevent the exacerbation of kidney damage in MRL/lpr mice caused by ponatinib.

3.6. Ponatinib modulates adiponectin through the PDGFR/PI3K/AKT pathway

Building upon the bioinformatics analyses described above, our focus shifted to ADIPOQ. Initially, we examined the mRNA expression of *Adipoq* in renal tissues of MRL/lpr, C57, and MRL/MpJ mice (Fig. 7A). Notably, only MRL/lpr mice exhibited a significant increase in *Adipoq* mRNA expression following ponatinib administration, contrasting with MRL/lpr-H_2O. Conversely, *Adipoq* mRNA expression in the renal tissues of C57 and MRL/MpJ mice remain unaffected by ponatinib. Considering the diverse molecular isoforms of isoforms [25], it's noteworthy that high molecular weight (HMW) ADIPOQ has pro-inflammatory effects [26]. To further investigate this aspect, we proceed to quantify HMW ADIPOQ in the kidneys of MRL/lpr-H_2O and MRL/lpr-PONA mice using non-denaturing gel electrophoresis (Fig. 7B). The results demonstrated a significant increase in HMW ADIPOQ content in MRL/lpr mice treated ponatinib compared to those treated ddH_2O ($p < 0.05$).

To explore the pathways through which ponatinib influences ADIPOQ, we performed a Protein-Protein Interaction (PPI) analysis of ADIPOQ and PDGFR using STRING (results as in Fig. 7E). The analysis revealed a close interaction between ADIPOQ and PDGFR. Research has shown that PDGFR is a marker for adipocyte progenitor cells (AP) [27], and it has been found that PDGFRα/PDGFRβ play an important role in the differentiation of AP into adipocytes. The inhibition of either PDGFRα or PDGFRβ can induce the formation of adipocytes [28]. Additionally, studies have indicated that the transformation of AP into adipocytes is related to a decrease in the phosphorylation level of PDGFRα. Inhibition of PDGFRα phosphorylation leads to reduced phosphorylation levels of its downstream PI3K/Akt pathway [29], which promotes the generation of adipocytes.

To investigate whether ponatinib affects the PDGFR/PI3K/AKT pathway, we examined the phosphorylation levels of PDGFRα (Tyr754) and AKT (Ser 473) in the renal tissues of MRL/lpr-H_2O and MRL/lpr-PONA mice (Fig. 7C and D). The results indicated a reduction in the levels of p-PDGFRα (Tyr754) and p-AKT (Ser 473) after ponatinib administration. Thus, by inhibiting the phosphorylation of PDGFRα and

Table 1
7 genes with greater than 20-fold expression in DEGs.

Gene name	FoldChange	pvalue	function	Clinical biomarker
Ucp1	108.8219161	2.14E-08	Mitochondrial Uncoupling Proteins (UCPs) are part of the mitochondrial anion carrier protein (MACP) family. They aid in transferring anions from the inner to the outer mitochondrial membrane and facilitating the reverse transfer of protons.	
Retnla	68.61017428	0.000191801	Proteins involved in the maintenance of calcium ion homeostasis within cells. They bind retinol and other retinoids, participating in the transport and storage of retinoids.	
Sprr2g	27.88763708	2.80E-05	Involved in sperm formation and may affect fertility.	
Adipoq	25.72156294	1.06E-08	A protein secreted by adipose cells that is associated with various physiological processes including metabolism of glucose and lipids, as well as anti-inflammatory and anti-atherosclerotic effects.	Yes [46,47]
Cma1	23.40499145	3.34E-05	It is found in mast cells and is believed to play a role in breaking down the extracellular matrix, regulating submucosal gland secretion, and producing vasoactive peptides.	
Lep	20.72211367	5.76E-05	This gene encodes a protein released into the bloodstream by white adipocytes, exerting a crucial role in governing energy homeostasis.	
Klrc1	0.030943868	4.35E-06	This gene encodes a protein that forms a complex with another family member, KLRD1/CD94, and is involved in the recognition of MHC class I HLA-E molecules by NK cells.	

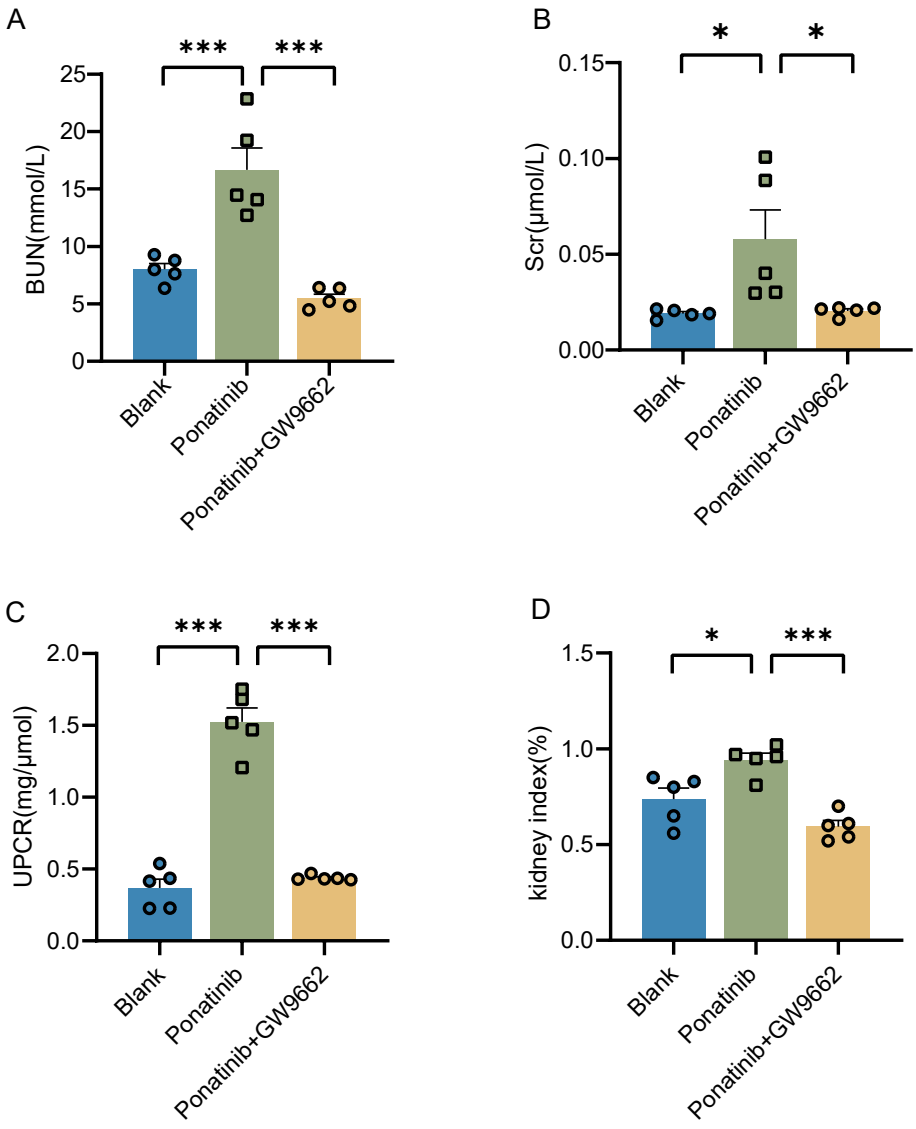

Fig. 6. After Blocking the Generation of Adiponectin, the Renal Injury Effect of Ponatinib on MRL/lpr Mice is Alleviated. (A) Blood urea nitrogen (B) Serum creatinine results (C) Urine protein-to-creatinine ratio (D) Kidney index after 2 weeks of ponatinib administration in the three mouse groups. The data are presented as the mean ± SEM. *p < 0.05; * *p < 0.01; * **p < 0.001.

AKT, ponatinib promoted the ADIPOQ expression, consequently contributing to renal injury.

4. Discussion

In this research, we have discovered the detrimental effects of ponatinib, a third-generation tyrosine kinase inhibitor, on lupus nephritis. Notably, the administration of ponatinib to MRL/lpr mice significantly exacerbated renal damage without causing changes in lupus-related autoimmune indicators. Specifically, administration of ponatinib to MRL/lpr mice resulted in a marked decline in renal function, accompanied by prominent acute pathological changes. However, markers such as dsDNA antibodies and ANA did not exhibit significant alterations. DsDNA antibodies are specific to SLE and have significant diagnostic value for this condition. The presence of these antibodies is closely associated with the disease activity of lupus [30]. ANA have higher sensitivity but lower specificity. Therefore, in clinical diagnosis, the results of dsDNA antibodies are primarily relied upon for the diagnosis of lupus [31]. Additionally, we observed an increase in serum C3 levels; however, there was no significant change in the deposition of C3 immune complexes in the kidney. Typically, C3 levels can also increase during the acute phase of inflammation [32]. Therefore, considering these immune-related indicators collectively, we conclude that the kidney damage in mice following ponatinib intervention is not caused by immune factors. Further investigation revealed that the acute renal injury induced by ponatinib was specific to MRL/lpr mice compared to MRL/MpJ mice. Through RNA-seq analysis, we identified lipid metabolism-related pathways associated with renal injury. We also found that inhibiting ADIPOQ synthesis can alleviate the kidney damage caused by ponatinib in MRL/lpr mice. Additionally, we confirmed that ponatinib could impact the PI3K/AKT pathway through PDGFR, leading to changes in adiponectin and subsequently influencing the action of inflammatory factors.

Tyrosine kinase inhibitors (TKIs) are designed to selectively target overexpressed receptor tyrosine kinases (RTKs). Imatinib, as a first-generation TKI, has showing promising results in delaying proteinuria onset and preventing kidney damage in SLE mice model [8]. However, multiple studies indicate that various TKIs, including imatinib and ponatinib, are associated with a range of kidney injuries such as proteinuria, hypertension, and acute kidney injury [12,18,33–36].

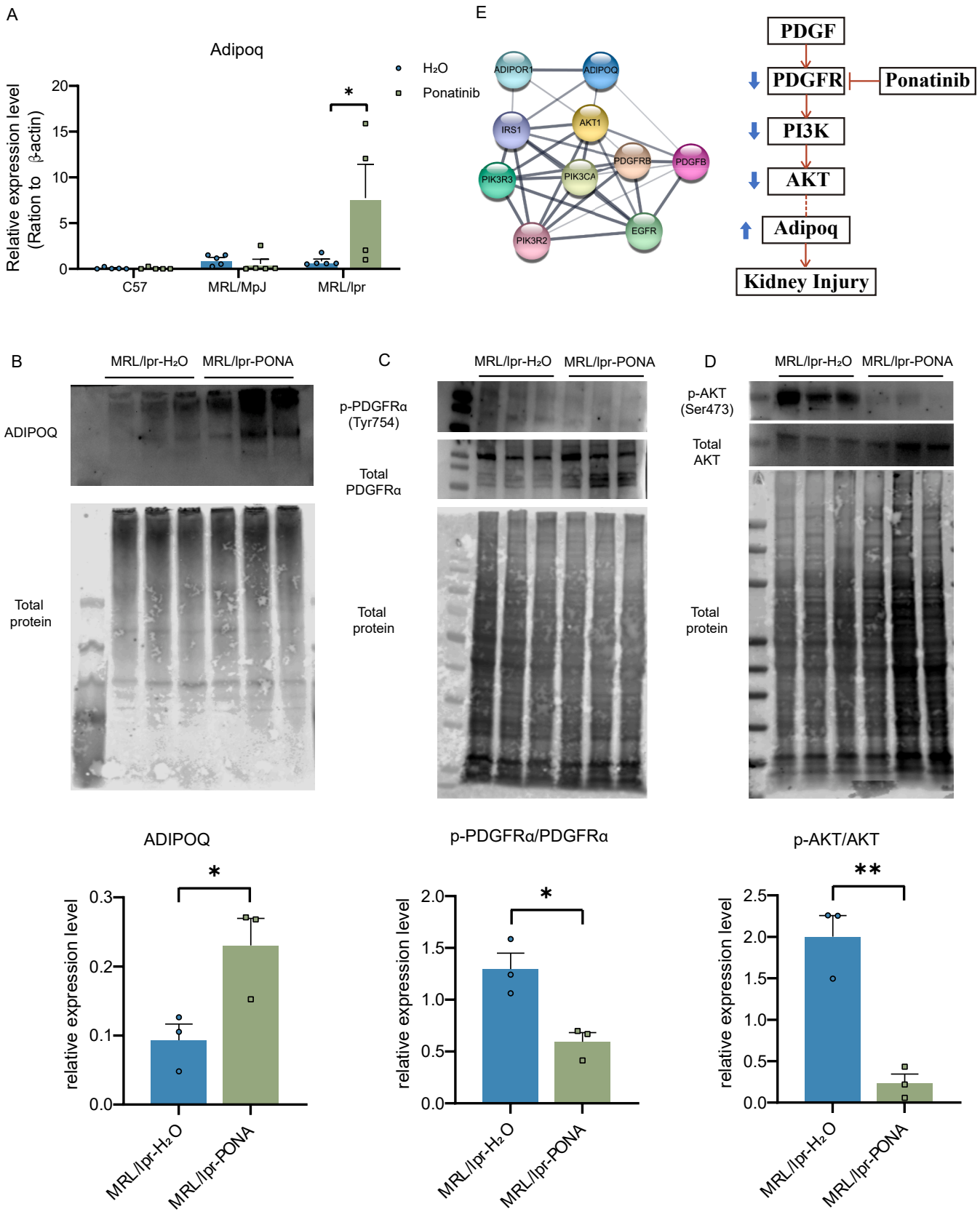

Fig. 7. Ponatinib Induces Renal Injury through the PDGFRβ-PI3K-Akt Pathway by Increasing High-Molecular-Weight Adiponectin Expression. (A) Renal adiponectin mRNA expression; (B) Renal ADIPOQ Western blot results; (C) Renal total-PDGFRα and p-PDGFRα(Tyr754) Western blot results; (D) Renal total-AKT and p-AKT (Ser473) Western blot results; (E) Protein-protein interaction prediction between ADIPOQ and PDGFR using String. The data are presented as the mean ± SEM. *$p < 0.05$; * *$p < 0.01$; * **$p < 0.001$ versus the corresponding control groups.

Adiponectin is a cytokine secreted by adipocytes, and under physiological conditions, it exerts anti-inflammatory, insulin-sensitizing, and anti-atherosclerotic effects. Adiponectin plays a role in glucose and lipid metabolism as well as energy balance. Adiponectin has two receptors, AdipoR1 and AdipoR2, with AdipoR1 widely expressed in intrinsic renal cells such as endothelial cells, podocytes, mesangial cells, and proximal tubular cells. The role of adiponectin in the kidneys is currently a subject of controversy. Previous studies have shown that elevated levels of adiponectin in the human population have been associated with a higher risk of end-stage renal disease and chronic kidney disease [37,38]. Higher adiponectin levels are also correlated with an increased risk of mortality [39]. Utilizing primary human Peripheral Blood Mononuclear Cells (PBMCs) and a microvascular endothelial cell line, researchers have discovered that HMW adiponectin promotes the production of Interleukin-8 (IL-8) and Monocyte Chemoattractant Protein-1 (MCP-1) in a dose-dependent manner, whereas low-molecular-weight (LMW) adiponectin does not exhibit such an effect. These two chemokines play pivotal roles in tissue inflammatory responses, suggesting that HMW adiponectin may hold significant importance in modulating inflammatory processes [26]. In rat models of chronic kidney failure, serum adiponectin levels increase [40]. In SLE patients with kidney involvement, significant elevations in blood, urine, and kidney adiponectin levels have been observed, and adiponectin levels are positively correlated with the severity of lupus nephritis [41,42]. Furthermore, in patients with rheumatoid arthritis [43,44] and inflammatory bowel disease [45], increased adipoq correlated with the severity of disease.

Our study suggests that ponatinib, a third-generation TKI, induces an upregulation of adiponectin and leads to acute kidney injury in lupus-prone mice by inhibiting the PDGFR-PI3K/AKT pathway. This ponatinib-induced acute kidney injury is unrelated to lupus autoimmune activity and has not been observed in other types of mice. The specificity of this effect on lupus-prone mice suggests a unique susceptibility of mouse kidneys to ponatinib in the context of lupus. It is essential to exercise caution when considering the use of ponatinib in patients with SLE, as our findings indicate a potential risk of kidney injury associated with its administration. Furthermore, given that systemic autoimmune diseases and chronic inflammatory diseases are characterized by increased secretion of adiponectin, it is imperative to exercise caution regarding the potential risks associated with using ponatinib.

Further validation of this conclusion is needed in additional animal models. Further studies are warranted to reveal the specific mechanism adiponectin leads to kidney damage and the cell type damaged by ponatinib. Further research and clinical investigations are also needed to better understand the mechanisms involved and to establish safety parameters for ponatinib use in lupus patients.

In summary, the study provides detailed insights into the specific effects of ponatinib on renal function, autoimmune markers, and molecular pathways in lupus-prone mice. The findings highlight the complexity of the drug's impact on different aspects of renal physiology and the potential involvement of lipid metabolism and inflammatory pathways.

These results highlight the necessity of vigilantly tracking renal function in individuals undergoing treatment with ponatinib.

5. Statement of ethics

This study protocol was reviewed and approved by the Experimental Animal Research of Peking Union Medical College (Approval number: ACUC-A01-2021–059).

Funding sources

This work is supported by the Chinese Academy of Medical Sciences Innovation Fund for Medical Sciences (2021- I2M-1—022), the CAMS Endowment Fund (2021-CAMS-JZ001), the Overseas Expertise Introduction Center for Discipline Innovation ("111Center") (BP0820029), the National Natural Science Foundation of China (81788101), Peking Union Scholars and Innovation Team Development Program (2016) and China National High Level Hospital Clinical Research Funding (2022-PUMCH-A-172).

CRediT authorship contribution statement

Yixin Dong: Writing – original draft, Visualization, Validation, Resources, Methodology, Investigation, Formal analysis, Data curation. **Gangan Wang:** Writing – original draft, Visualization, Validation, Resources, Methodology, Investigation, Formal analysis, Data curation. **Xiwei Yan:** Validation, Supervision, Project administration. **Wenling Ye:** Validation, Methodology. **Xiangyu Qiao:** Methodology, Formal analysis. **Xingyu Deng:** Validation. **Pengju Ren:** Validation, Investigation. **Chunyu Jia:** Validation. **Gang Chen:** Formal analysis. **Ke Zheng:** Writing – review & editing, Supervision. **Chengyu Jiang:** Writing – review & editing, Supervision, Resources, Project administration, Funding acquisition, Data curation, Conceptualization. **Xuemei Li:** Writing – review & editing, Supervision, Resources, Project administration, Funding acquisition, Data curation, Conceptualization.

Declaration of competing interest

The authors declare that they have no known competing financial interests or personal relationships that could have appeared to influence the work reported in this paper.

Acknowledgments

We would like to express our sincere gratitude to Weifang Cao from the Institute of Basic Medicine, Chinese Academy of Medical Sciences, Laboratory of Electron Microscopy, for providing technical assistance in capturing electron microscope images. We would like to express our sincere gratitude to State Key Laboratory of Common Mechanism Research for Major Diseases for providing State Key Laboratory Special Fund 2060204. Additionally, the "Graphical abstract" was created using HOME for Researchers (https://www.home-for-researchers.com). During the preparation of this work the authors used ChatGPT(https://chat.openai.com/) in order to refine the language and style of this manuscript. After using this tool, the authors reviewed and edited the content as needed and take full responsibility for the content of the publication.

Data availability

All data generated or analyzed during this study are included in this article. Further enquiries can be directed to the corresponding author.

References

[1] A. Davidson, What is damaging the kidney in lupus nephritis? Nat. Rev. Rheumatol. 12 (3) (2016) 143–153.
[2] M.R.W. Barber, C. Drenkard, T. Falasinnu, A. Hoi, A. Mak, N.Y. Kow, E. Svenungsson, J. Peterson, A.E. Clarke, R. Ramsey-Goldman, Global epidemiology of systemic lupus erythematosus, Nat. Rev. Rheumatol. 17 (9) (2021) 515–532.
[3] V. Tesar, Z. Hruskova, Treatment of proliferative lupus nephritis: a slowly changing landscape, Nat. Rev. Nephrol. 7 (2) (2011) 96–109.
[4] H.J. Anders, R. Saxena, M.H. Zhao, I. Parodis, J.E. Salmon, C. Mohan, Lupus nephritis, Nat. Rev. Dis. Primers 6 (1) (2020) 7.
[5] B.J. Druker, S. Tamura, E. Buchdunger, S. Ohno, G.M. Segal, S. Fanning, J. Zimmermann, N.B. Lydon, Effects of a selective inhibitor of the Abl tyrosine kinase on the growth of Bcr-Abl positive cells, Nat. Med. 2 (5) (1996) 561–566.
[6] K.P. Szilveszter, T. Németh, A. Mócsai, Tyrosine kinases in autoimmune and inflammatory skin diseases, Front. Immunol. 10 (2019) 1862.
[7] B.J. Skaggs, B.H. Hahn, L. Sahakian, J. Grossman, M. McMahon, Dysfunctional, pro-inflammatory HDL directly upregulates monocyte PDGFRβ, chemotaxis and TNFα production, Clin. Immunol. 137 (1) (2010) 147–156.
[8] C. Zoja, D. Corna, D. Rottoli, C. Zanchi, M. Abbate, G. Remuzzi, Imatinib ameliorates renal disease and survival in murine lupus autoimmune disease, Kidney Int. 70 (1) (2006) 97–103.

[9] L. Yang, T. Zhang, P. Wang, W. Chen, W. Liu, X. He, Y. Zhang, S. Jin, Z. Luo, Z. Zhang, X. Wang, J. Liu, Imatinib and M351–0056 enhance the function of VISTA and ameliorate the development of SLE via IFN-I and noncanonical NF-κB pathway, Cell Biol. Toxicol. 39 (6) (2023) 3287–3304.
[10] A. Sadanaga, H. Nakashima, K. Masutani, K. Miyake, S. Shimizu, T. Igawa, N. Sugiyama, H. Niiro, H. Hirakata, M. Harada, Amelioration of autoimmune nephritis by imatinib in MRL/lpr mice, Arthritis Rheum. 52 (12) (2005) 3987–3996.
[11] Q. Fan, J. Ma, B. Zhang, Q. Li, F. Liu, B. Zhao, Assessment of acute kidney injury related to small-molecule protein kinase inhibitors using the FDA adverse event reporting system, Cancer Chemother. Pharmacol. 86 (5) (2020) 655–662.
[12] M. Cellier, D. Bourneau-Martin, C. Abbara, A. Crosnier, L. Lagarce, A.S. Garnier, M. Briet, Renal safety profile of BCR-ABL tyrosine kinase inhibitors in a real-life setting: a study based on Vigibase(®), the WHO pharmacovigilance database, Cancers (Basel) 15 (7) (2023).
[13] A. Abbas, M.M. Mirza, A.K. Ganti, K. Tendulkar, Renal toxicities of targeted therapies, Target. Oncol. 10 (4) (2015) 487–499.
[14] A. Hulin, T. Gelé, C. Fenioux, E. Kempf, D. Sahali, C. Tournigand, M. Ollero, Pharmacology of tyrosine kinase inhibitors: implications for patients with kidney diseases, Clin. J. Am. Soc. Nephrol. 19 (7) (2023) 927–938.
[15] E. Lierman, S. Smits, J. Cools, B. Dewaele, M. Debiec-Rychter, P. Vandenberghe, Ponatinib is active against imatinib-resistant mutants of FIP1L1-PDGFRA and KIT, and against FGFR1-derived fusion kinases, Leukemia 26 (7) (2012) 1693–1695.
[16] I. Sadovnik, E. Lierman, B. Peter, H. Herrmann, V. Suppan, G. Stefanzl, O. Haas, T. Lion, W. Pickl, J. Cools, P. Vandenberghe, P. Valent, Identification of Ponatinib as a potent inhibitor of growth, migration, and activation of neoplastic eosinophils carrying FIP1L1-PDGFRA, Exp. Hematol. 42 (4) (2014) 282–293.e4.
[17] H.M. Kantarjian, E. Jabbour, M. Deininger, E. Abruzzese, J. Apperley, J. Cortes, C. Chuah, D.J. DeAngelo, J. DiPersio, A. Hochhaus, J. Lipton, F.E. Nicolini, J. Pinilla-Ibarz, D. Rea, G. Rosti, P. Rousselot, N.P. Shah, M. Talpaz, S. Srivastava, X. Ren, M. Mauro, Ponatinib after failure of second-generation tyrosine kinase inhibitor in resistant chronic-phase chronic myeloid leukemia, Am. J. Hematol. 97 (11) (2022) 1419–1426.
[18] M. Stanchina, Z. McKinnell, J.H. Park, E.M. Stein, S.F. Cai, J. Taylor, BCR-ABL tyrosine kinase inhibitor (TKI)-induced nephropathy: an under-recognized phenomenon, Leuk Res. Rep. 14 (2020) 100211.
[19] T. O'Hare, W.C. Shakespeare, X. Zhu, C.A. Eide, V.M. Rivera, F. Wang, L.T. Adrian, T. Zhou, W.S. Huang, Q. Xu, C.A. Metcalf 3rd, J.W. Tyner, M.M. Loriaux, A. S. Corbin, S. Wardwell, Y. Ning, J.A. Keats, Y. Wang, R. Sundaramoorthi, M. Thomas, D. Zhou, J. Snodgrass, L. Commodore, T.K. Sawyer, D.C. Dalgarno, M. W. Deininger, B.J. Druker, T. Clackson, AP24534, a pan-BCR-ABL inhibitor for chronic myeloid leukemia, potently inhibits the T315I mutant and overcomes mutation-based resistance, Cancer Cell 16 (5) (2009) 401–412.
[20] S.E. Choi, A.B. Fogo, B.J. Lim, Histologic evaluation of activity and chronicity of lupus nephritis and its clinical significance, Kidney Res. Clin. Pract. 42 (2) (2023) 166–173.
[21] X. Qiao, F. Huang, X. Shi, X. Deng, C. Zhang, S. Mei, Z. Wang, C. Zhou, C. Jiang, X. Tan, Herbal small RNAs in patients with COVID-19 linked to reduced DEG expression, Sci. China Life Sci. 66 (6) (2023) 1280–1289.
[22] M. Al, L. Ng, P. Tyrrell, J. Bargman, T. Bradley, E. Silverman, Adipokines as novel biomarkers in paediatric systemic lupus erythematosus, Rheumatology (Oxford) 48 (5) (2009) 497–501.
[23] M.Y. Zhang, A.A. Dini, X.K. Yang, L.J. Li, G.C. Wu, R.X. Leng, H.F. Pan, D.Q. Ye, Association between serum/plasma adiponectin levels and immune-mediated diseases: a meta-analysis, Arch. Dermatol. Res. 309 (8) (2017) 625–635.
[24] M. Guo, C. Li, Y. Lei, S. Xu, D. Zhao, X.Y. Lu, Role of the adipose PPARγ-adiponectin axis in susceptibility to stress and depression/anxiety-related behaviors, Mol. Psychiatry 22 (7) (2017) 1056–1068.
[25] É. Toussirot, D. Binda, C. Gueugnon, G. Dumoulin, Adiponectin in autoimmune diseases, Curr. Med. Chem. 19 (32) (2012) 5474–5480.
[26] H. Song, J. Chan, B.H. Rovin, Induction of chemokine expression by adiponectin in vitro is isoform dependent, Transl. Res. 154 (1) (2009) 18–26.
[27] Z. Gao, A.C. Daquinag, F. Su, B. Snyder, M.G. Kolonin, PDGFRα/PDGFRβ signaling balance modulates progenitor cell differentiation into white and beige adipocytes, Development 145 (1) (2018).
[28] C. Sun, H. Sakashita, J. Kim, Z. Tang, G.M. Upchurch, L. Yao, W.L. Berry, T. M. Griffin, L.E. Olson, Mosaic mutant analysis identifies PDGFRα/PDGFRβ as negative regulators of adipogenesis, Cell Stem Cell 26 (5) (2020) 707–721.e5.
[29] S. Fitter, K. Vandyke, S. Gronthos, A.C. Zannettino, Suppression of PDGF-induced PI3 kinase activity by imatinib promotes adipogenesis and adiponectin secretion, J. Mol. Endocrinol. 48 (3) (2012) 229–240.
[30] M.E. Orme, A. Voreck, R. Aksouh, R. Ramsey-Goldman, M.W.J. Schreurs, Systematic review of anti-dsDNA testing for systemic lupus erythematosus: a meta-analysis of the diagnostic test specificity of an anti-dsDNA fluorescence enzyme immunoassay, Autoimmun. Rev. 20 (11) (2021) 102943.
[31] M. Aringer, K. Costenbader, D. Daikh, R. Brinks, M. Mosca, R. Ramsey-Goldman, J. S. Smolen, D. Wofsy, D.T. Boumpas, D.L. Kamen, D. Jayne, R. Cervera, N. Costedoat-Chalumeau, B. Diamond, D.D. Gladman, B. Hahn, F. Hiepe, S. Jacobsen, D. Khanna, K. Lerstrøm, E. Massarotti, J. McCune, G. Ruiz-Irastorza, J. Sanchez-Guerrero, M. Schneider, M. Urowitz, G. Bertsias, B.F. Hoyer, N. Leuchten, C. Tani, S.K. Tedeschi, Z. Touma, G. Schmajuk, B. Anic, F. Assan, T.M. Chan, A.E. Clarke, M. K. Crow, L. Czirják, A. Doria, W. Graninger, B. Halda-Kiss, S. Hasni, P.M. Izmirly, M. Jung, G. Kumánovics, X. Mariette, I. Padjen, J.M. Pego-Reigosa, J. Romero-Diaz, Í. Rúa-Figueroa Fernández, R. Seror, G.H. Stummvoll, Y. Tanaka, M.G. Tektonidou, C. Vasconcelos, E.M. Vital, D.J. Wallace, S. Yavuz, P.L. Meroni, M.J. Fritzler, R. Naden, T. Dörner, S.R. Johnson, 2019 European League Against Rheumatism/American College of Rheumatology classification criteria for systemic lupus erythematosus, Ann Rheum Dis 78(9) (2019) 1151-1159.
[32] A. Zarantonello, M. Revel, A. Grunenwald, L.T. Roumenina, C3-dependent effector functions of complement, Immunol. Rev. 313 (1) (2023) 120–138.
[33] K.D. Jhaveri, V. Sakhiya, R. Wanchoo, D. Ross, S. Fishbane, Renal effects of novel anticancer targeted therapies: a review of the food and drug administration adverse event reporting system, Kidney Int. 90 (3) (2016) 706–707.
[34] H. François, P. Coppo, J.P. Hayman, B. Fouqueray, B. Mougenot, P. Ronco, Partial fanconi syndrome induced by imatinib therapy: a novel cause of urinary phosphate loss, Am. J. Kidney Dis. 51 (2) (2008) 298–301.
[35] P. Kandula, R. Agarwal, Proteinuria and hypertension with tyrosine kinase inhibitors, Kidney Int. 80 (12) (2011) 1271–1277.
[36] K.D. Jhaveri, R. Wanchoo, V. Sakhiya, D.W. Ross, S. Fishbane, Adverse renal effects of novel molecular oncologic targeted therapies: a narrative review, Kidney Int. Rep. 2 (1) (2017) 108–123.
[37] I.C. Kuo, P.H. Wu, H.Y. Lin, S.W. Niu, J.C. Huang, C.C. Hung, Y.W. Chiu, H. C. Chen, The association of adiponectin with metabolic syndrome and clinical outcome in patients with non-diabetic chronic kidney disease, PLoS One 14 (7) (2019) e0220158.
[38] S.H. Song, T.R. Oh, H.S. Choi, C.S. Kim, S.K. Ma, K.H. Oh, C. Ahn, S.W. Kim, E. H. Bae, High serum adiponectin as a biomarker of renal dysfunction: results from the KNOW-CKD study, Sci. Rep. 10 (1) (2020) 5598.
[39] C.M. Rhee, D.V. Nguyen, H. Moradi, S.M. Brunelli, R. Dukkipati, J. Jing, T. Nakata, C.P. Kovesdy, G.A. Brent, K. Kalantar-Zadeh, Association of adiponectin with body composition and mortality in hemodialysis patients, Am. J. Kidney Dis. 66 (2) (2015) 313–321.
[40] Y. Yu, B.J. Bao, Y.P. Fan, L. Shi, S.Q. Li, Changes of adiponectin and its receptors in rats following chronic renal failure, Ren. Fail. 36 (1) (2014) 92–97.
[41] B.H. Rovin, H. Song, L.A. Hebert, T. Nadasdy, G. Nadasdy, D.J. Birmingham, C. Yung Yu, H.N. Nagaraja, Plasma, urine, and renal expression of adiponectin in human systemic lupus erythematosus, Kidney Int. 68 (4) (2005) 1825–1833.
[42] S.M. Kamel, M. Abdel Azeem Abd Elazeem, R.A. Mohamed, M.M. Kamel, E. A. Abdel Aleem Abdelaleem, High serum leptin and adiponectin levels as biomarkers of disease progression in Egyptian patients with active systemic lupus erythematosus, Int. J. Immunopathol. Pharmacol. 37 (2023), 3946320231154988.
[43] U. Müller-Ladner, E. Neumann, Rheumatoid arthritis: the multifaceted role of adiponectin in inflammatory joint disease, Nat. Rev. Rheumatol. 5 (12) (2009) 659–660.
[44] D. Liu, S. Luo, Z. Li, Multifaceted roles of adiponectin in rheumatoid arthritis, Int. Immunopharmacol. 28 (2) (2015) 1084–1090.
[45] H.S.H. Al-Khalidy, R.M. Hasan, B.M. Mahdi, Role of adiponectin in patients with inflammatory bowel disease unclassified, Journal of Coloproctology 38 (4) (2018) 320–323.
[46] H.I. Brunner, G. Gulati, M.S. Klein-Gitelman, K.A. Rouster-Stevens, L. Tucker, S. P. Ardoin, K.B. Onel, R. Mainville, J. Turnier, P.O.A. Aydin, D. Witte, B. Huang, M. R. Bennett, P. Devarajan, Urine biomarkers of chronic kidney damage and renal functional decline in childhood-onset systemic lupus erythematosus, Pediatr. Nephrol. 34 (1) (2019) 117–128.
[47] M. Loghman, A. Haghighi, B. Broumand, Y. Ataipour, M. Tohidi, C. Marzbani, M. Fakharran, Association between urinary adiponectin level and renal involvement in systemic lupus erythematous, Int. J. Rheum. Dis. 19 (7) (2016) 678–684.